Nonlinear Marangoni convection with the inclined temperature gradient in multilayer systems

I. Simanovskii,[1] A. Nepomnyashchy,[1] V. Shevtsova,[2] P. Colinet,[2] and J.-C. Legros[2]
[1]*Department of Mathematics, Technion—Israel Institute of Technology, 32000 Haifa, Israel*
[2]*Service de Chimie Physique EP, Universiteé Libré de Bruxelles, Code Postal 165-62, 50 Avenue F. D. Roosevelt 1050, Brussels, Belgium*
(Received 3 January 2006; revised manuscript received 22 May 2006; published 29 June 2006)

The influence of the horizontal component of the temperature gradient on nonlinear regimes of oscillatory Marangoni convection in a real symmetric three-layer system is investigated. The transitions between different flow regimes have been studied. The general diagram of regimes is constructed.

DOI: 10.1103/PhysRevE.73.066310 PACS number(s): 47.55.pf

I. INTRODUCTION

Prediction of fluid behavior under microgravity conditions is an important problem in space engineering. Experiments in space revealed the dominant role of the thermocapillary convection in microgravity fluid dynamics. The case when the system has only one interface between different fluids has been studied analytically and numerically in many works (see, for example, the monograph [1]). Convection in a system with one interface and one free surface was considered in [2].

During the last decade, a new scientific direction of investigation, convection in multilayer systems, was developed. The interest in such systems is caused first of all by various technological applications. Among the modern techniques requiring an investigation of convection in systems with many interfaces are liquid encapsulation crystal growth technique [3,4] used in Spacelab missions, droplet-droplet coalescence processes, where Marangoni convection in the interdroplet film can considerably affect the coalescence time during extraction [5], and others. The scientific interest in such systems is due to the fact that the interfacial convection in multilayer systems is characterized by a variety of physical mechanisms and types of instability. The understanding of the underlying physical processes that can be achieved through the exploration of the mutual influence and the interaction between different interfaces is necessary for a successful application of this phenomenon. Simultaneous interaction of interfaces with their bulk phases and with each other was studied on heating from below and from above [6,7], as well as in the case of horizontal temperature gradients [8–11].

Numerical investigations of thermocapillary convection in multilayer systems were started in [12–14]. In these papers the linear stability of the mechanical equilibrium state and the nonlinear regimes of convection for a system of three immiscible viscous fluids were studied. In particular, in [12,14] it was shown that a symmetric three-layer configuration may become unstable with respect to oscillatory disturbances when one fluid is sandwiched between two layers of another fluid. This specific mechanism of instability is caused by the interaction between the two interfaces. An analysis of different mechanisms of direct and indirect interaction between Rayleigh and thermocapillary instabilities in real three-layer systems was given in [7]. It was shown that the oscillatory mechanism of instability in a three-layer system is much more widespread than in a two-layer one.

Experimental results on the Marangoni-Benard instability under microgravity conditions have been described in [15,16]. A microgravity experiment, devoted to the instability of a liquid system with close thermal diffusivities, *n*-octane–methanol–*n*-octane, was performed on the LMS mission of Spacelab onboard the U.S. Space Shuttle [16]. The experimental results confirm the existence of an oscillatory instability, essentially connected with the interaction of the interfaces, in coincidence with the predictions of linear stability theory [16].

Under experimental conditions, the temperature gradient in the system is not perfectly vertical and a horizontal component of the temperature gradient appears. The appearance of this component changes the situation completely: even for small values of the Marangoni number ($M \neq 0$), the mechanical equilibrium state becomes impossible in principle, and a convective flow takes place in the system. The influence of this flow on the convective patterns generated by the vertical temperature gradient in two-layer systems has been investigated in detail in the case of the usual Rayleigh-Benard convection (see [17–19]). The stability of thermocapillary flows with an inclined temperature gradient was studied in [20,21]. Nonlinear simulations of convective flows in a closed cavity filled by a symmetric three-layer system in the case where the temperature gradient is directed along the interfaces were considered in [22]. The interaction between the convection caused by the temperature gradient directed perpendicularly to the interfaces and the convective flow produced by the horizontal component of the temperature gradient in three-layer systems has not been studied to our knowledge.

In the present paper, we investigate the influence of the horizontal component of the temperature gradient on nonlinear regimes of oscillatory Marangoni convection that are developed in the 47v2 silicone oil–water–47v2 silicone oil system. Transitions between convective flows are studied numerically.

In Sec. II, the mathematical formulation of the problem and the numerical method are presented. Section III is devoted to the consideration of flows generated by the joint action of the vertical and horizontal components of the temperature gradient. Section IV contains some concluding remarks.

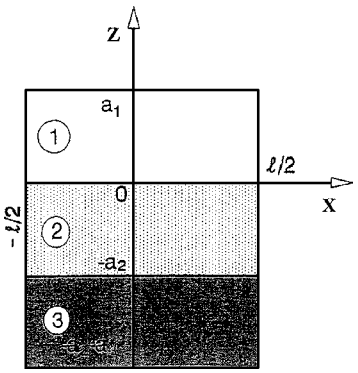

FIG. 1. Geometrical configuration of the system and coordinate axes.

II. GENERAL EQUATIONS AND BOUNDARY CONDITIONS

Let the space between two parallel rigid horizontal plates be filled by three immiscible viscous fluids (see Fig. 1). The physical properties of layer 1 (the top layer) and layer 3 (the bottom layer) are identical, whereas those of layer 2 (the middle layer) are different. The equilibrium thickness of each layer is a. We assume that the deformations of interfaces are small, and their influence on the flow and temperature distribution can be ignored. The surface tension coefficient σ is a linear function of temperature T: $\sigma=\sigma_0-\alpha T$. We do not take into account buoyancy effects which are negligible in the case of thin layers or under microgravity conditions. The temperature on the horizontal plates $z=a_1$ and $z=-a_2-a_3$ is fixed in the following way: $T(x,z,a_1)=-A_h x$, $T(x,z,-a_2-a_3)=-A_h x+\theta$, $A_h>0$. The vertical lateral boundaries $x=0$ and $x=l$ are heat insulated. Let us use the following notations:

$$\rho=\rho_1/\rho_2, \quad \nu=\nu_1/\nu_2, \quad \eta=\eta_1/\eta_2, \quad \kappa=\kappa_1/\kappa_2, \quad \chi=\chi_1/\chi_2, a=a_2/a_1.$$

Here ρ_m, ν_m, η_m, κ_m, χ_m, and a_m are, respectively, the density, the kinematic and the dynamic viscosity, the heat conductivity, the thermal diffusivity, and the thickness of the mth layer ($m=1,2$). As the units of length, time, velocity, pressure, and temperature we use a, a^2/ν_1, ν_1/a, $\rho_1\nu_1^2/a^2$, and θ, respectively. The complete nonlinear equations governing the Marangoni convection (see [1]) have the following form:

$$\frac{\partial \mathbf{v}_m}{\partial t}+(\mathbf{v}_m\cdot\boldsymbol{\nabla})\mathbf{v}_m=-e_m\boldsymbol{\nabla}p_m+c_m\Delta\mathbf{v}_m, \tag{1}$$

$$\frac{\partial T_m}{\partial t}+\mathbf{v}_m\cdot\boldsymbol{\nabla}T_m=\frac{d_m}{P}\Delta T_m, \tag{2}$$

$$\boldsymbol{\nabla}\cdot\mathbf{v}_m=0. \tag{3}$$

Here, $e_1=c_1=d_1=1$, $e_2=\rho$, $c_2=1/\nu$, and $d_2=1/\chi$.

The conditions on the rigid horizontal boundaries are

$$v_1=0, \quad T_1=-\epsilon x, \quad (z=1), \tag{4}$$

$$v_3=0, \quad T_3=-\epsilon x+1, \quad (z=-2), \tag{5}$$

where $\epsilon=A_h a_1/\theta>0$ is the nondimensional parameter characterizing the horizontal component of the temperature gradient. The boundary conditions on the interface $z=0$ can be written in the form

$$\eta\frac{\partial v_{1x}}{\partial z}-\frac{\partial v_{2x}}{\partial z}-\frac{\eta M}{P}\frac{\partial T_1}{\partial x}=0, \quad \eta\frac{\partial v_{1y}}{\partial z}-\frac{\partial v_{2y}}{\partial z}-\frac{\eta M}{P}\frac{\partial T_1}{\partial y}=0, \tag{6}$$

$$v_{1x}=v_{2x}, \quad v_{1y}=v_{2y}, \quad v_{1z}=v_{2z}, \tag{7}$$

$$T_1=T_2, \tag{8}$$

$$\kappa\frac{\partial T_1}{\partial z}=\frac{\partial T_2}{\partial z}; \tag{9}$$

and at $z=-1$,

$$\eta^{-1}\frac{\partial v_{2x}}{\partial z}-\frac{\partial v_{3x}}{\partial z}-\frac{M}{P}\frac{\partial T_2}{\partial x}=0, \quad \eta^{-1}\frac{\partial v_{2y}}{\partial z}-\frac{\partial v_{3y}}{\partial z}-\frac{M}{P}\frac{\partial T_2}{\partial y}=0, \tag{10}$$

$$v_{2x}=v_{3x}, \quad v_{2y}=v_{3y}, \quad v_{2z}=v_{3z}, \tag{11}$$

$$T_2=T_3, \tag{12}$$

$$\kappa^{-1}\frac{\partial T_2}{\partial z}=\frac{\partial T_3}{\partial z}. \tag{13}$$

Here $P=\nu_1/\chi_1$ is the Prandtl number for the liquid in layer 1 and $M=\alpha\theta a/\eta_1\chi_1$ is the Marangoni number.

The conditions on the solid lateral boundaries, which are assumed to be thermally insulated, are

$$v_m=0, \quad \frac{\partial T_m}{\partial x}=0, \quad m=1,2,3 \quad (x=0,L). \tag{14}$$

The above mentioned boundary value problem in the case $\epsilon=0$ has a solution

$$v_m=0, \quad p_m=0, \quad m=1,2,3, \tag{15}$$

$$T_1=T_1^0=-\frac{(z-1)}{2+\kappa}, \tag{16}$$

$$T_2=T_2^0=-\frac{(\kappa z-1)}{2+\kappa}, \tag{17}$$

$$T_3=T_3^0=-\frac{(z-1)+(1-\kappa)}{2+\kappa}, \tag{18}$$

corresponding to the mechanical equilibrium state. Depending on the physical parameters of the fluids, the mechanical equilibrium state may become unstable with respect to different instability modes. In the case $\epsilon\neq 0$, the mechanical equilibrium is impossible in principle and the convective motion appears in the system.

III. NUMERICAL SIMULATIONS

In this section, we present the results of the nonlinear numerical solution of the boundary value problem (1)–(13) for the system 47v2 silicone oil–water–47v2 silicone oil with the following set of parameters: $\eta=1.7375$, $\nu=2$, $\kappa=0.184$, $\chi=0.778$, $\eta_*=\nu_*=\kappa_*=\chi_*=1$, $P=25.7$. We take $a=a_*=1$. It means that the exterior layers have the same thermophysical properties. For two-dimensional flows ($v_{my}=0$; the fields of physical variables do not depend on y), we can introduce the stream function ψ_m and the vorticity ϕ_m,

$$v_{m,x}=\frac{\partial\psi_m}{\partial z},\quad v_{m,z}=-\frac{\partial\psi_m}{\partial x},\quad \phi_m=\frac{\partial v_{m,z}}{\partial x}-\frac{\partial v_{m,x}}{\partial z}$$

$$(m=1,2,3),$$

and rewrite Eqs. (1)–(3) in the following form:

$$\frac{\partial\phi_m}{\partial t}+\frac{\partial\psi_m}{\partial z}\frac{\partial\phi_m}{\partial x}-\frac{\partial\psi_m}{\partial x}\frac{\partial\phi_m}{\partial z}=d_m\Delta\phi_m, \tag{19}$$

$$\Delta\psi_m=-\phi_m, \tag{20}$$

$$\frac{\partial T_m}{\partial t}+\frac{\partial\psi_m}{\partial z}\frac{\partial T_m}{\partial x}-\frac{\partial\psi_m}{\partial x}\frac{\partial T_m}{\partial z}=\frac{c_m}{P}\Delta T_m\quad (m=1,2,3). \tag{21}$$

At the interfaces the boundary conditions read, for $z=0$,

$$\psi_1=\psi_2=0,\quad \frac{\partial\psi_1}{\partial z}=\frac{\partial\psi_2}{\partial z},\quad T_1=T_2, \tag{22}$$

$$\frac{\partial T_1}{\partial z}=\frac{1}{\kappa}\frac{\partial T_2}{\partial z},\quad \frac{\partial^2\psi_1}{\partial z^2}=\frac{1}{\eta}\frac{\partial^2\psi_2}{\partial z^2}+\frac{M}{P}\frac{\partial T_1}{\partial x}, \tag{23}$$

and for $z=-1$,

$$\psi_2=\psi_3=0,\quad \frac{\partial\psi_2}{\partial z}=\frac{\partial\psi_3}{\partial z},\quad T_2=T_3, \tag{24}$$

$$\frac{1}{\kappa}\frac{\partial T_2}{\partial z}=\frac{\partial T_3}{\partial z},\quad \frac{1}{\eta}\frac{\partial^2\psi_2}{\partial z^2}=\frac{\partial^2\psi_3}{\partial z^2}+\frac{M}{P}\frac{\partial T_2}{\partial x}. \tag{25}$$

On the horizontal solid plates, for $z=1$,

$$\psi_1=\frac{\partial\psi_1}{\partial z}=0,\quad T_1=-\epsilon x, \tag{26}$$

and for $z=-2$,

$$\psi_3=\frac{\partial\psi_3}{\partial z}=0,\quad T_3=-\epsilon x+1. \tag{27}$$

On the solid heat-insulated lateral walls, for $x=0,L$,

$$\psi_m=\frac{\partial\psi_m}{\partial x}=\frac{\partial T_m}{\partial x}=0\quad (m=1,2,3). \tag{28}$$

The boundary value problem formulated above was solved by the finite-difference method. Equations were approximated on a uniform mesh using a second-order approximation for the spatial coordinates. The calculations were started with initial conditions corresponding to equilibrium fields of temperature and localized vorticity of different signs in several points. Equations were solved using the explicit scheme on a rectangular uniform 42×84 mesh. The Poisson equations were solved by the iterative Liebman successive overrelaxation method on each time step: the accuracy of the solution was 10^{-5}. The nonlinear simulations have been performed for $L=3.2$. The details of the method may be found in [1].

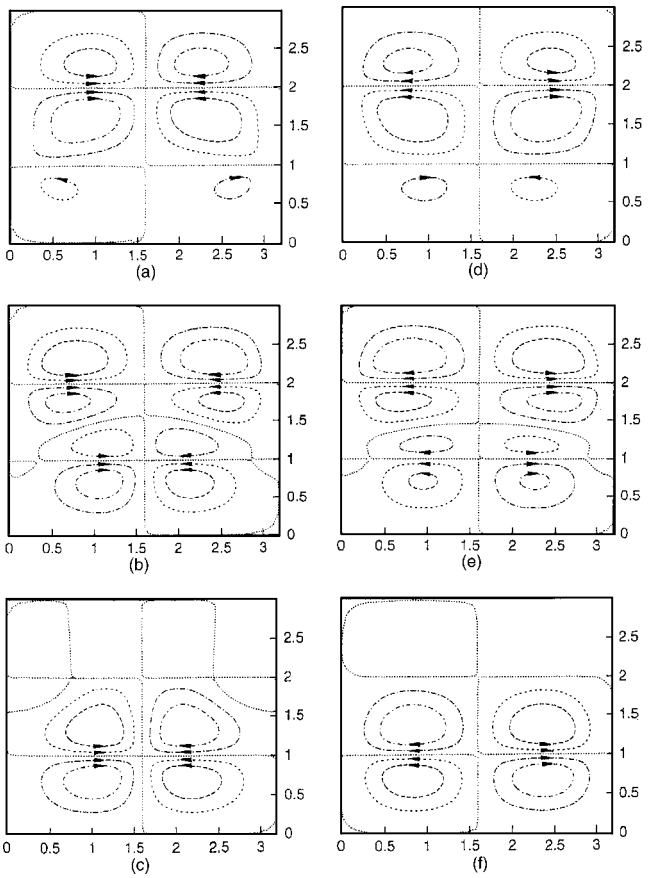

FIG. 2. (a)–(f) Streamlines for periodic oscillatory motion ($\epsilon=0$; $M=25\,000$).

A. The case $\epsilon=0$

According to the nonlinear simulations, the mechanical equilibrium state is stable if $M\leqslant M_c^n=12\,400$. As $M\geqslant M_c^n$, the equilibrium state becomes unstable with respect to oscillatory disturbances.

Let us describe qualitatively the flow evolution during the period of oscillations $0<t<\tau$ (see Fig. 2). For any values of t, the fields of stream function and temperature satisfy the symmetry conditions

$$\psi_m(x,z,t)=-\psi_m(-x,z,t),\quad T_m(x,z,t)=T_m(-x,z,t),$$

$$m=1,2,3. \tag{29}$$

We start from the state where an intensive thermocapillary convection takes place mainly in the top and middle layers,

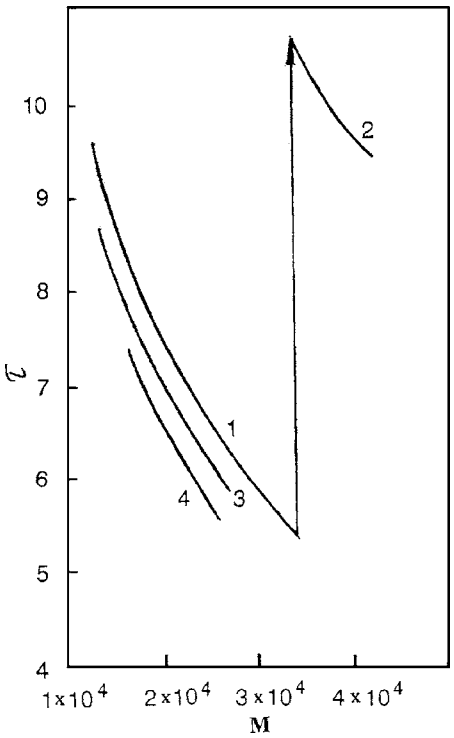

FIG. 3. The dependence of the oscillation period τ on the Marangoni number M; $\epsilon=0$ (lines 1, 2); $\epsilon=0.045$ (line 3); $\epsilon=0.085$ (line 4).

while the fluid in the bottom layer is almost stagnant [Fig. 2(a)]. The fluid motion in the middle layer induces two weak vortices in the bottom layer. Because the descending flow in the center of the middle layer is more intense than the ascending flow in the bottom layer, a minimum of the temperature distribution appears at the central point of the lower interface. As a result, the thermocapillary stresses on the lower interface generate a new four-vortex structure, which consists of two vortices in the bottom layer and two vortices in the middle layer [see Fig. 2(b)]. A "two-storey" structure appears in the middle layer. Eventually, the new vortices oust the former ones in the middle layer. The intense motion developing in the middle layer induces a motion in the opposite direction in the top layer [Fig. 2(c)] and diminishes the temperature in the center of the lower interface. Because of the latter phenomenon, the motion in the bottom layer slows down [Fig. 2(d)] and changes its direction [Fig. 2(e)]. A two-storey structure appears again in the middle layer. Note that after half a period $\tau/2$ the structure coincides with the initial one but it is shifted by the distance $L/2$ in the horizontal direction:

$$\psi_m(x,z,t+\tau/2) = \psi_m(x+L/2,z,t),$$

$$T_m(x,z,t+\tau/2) = T_m(x+L/2,z,t), \quad m=1,2,3. \tag{30}$$

The new growing vortices in the middle layer suppress the upper pair of vortices [Fig. 2(f)], enhance the temperature near the sidewalls on the upper interface, and diminish the temperature in the center of the lower interface. That is why the flow in the bottom layer is suppressed, and finally the structure returns to the configuration of Fig. 2(a).

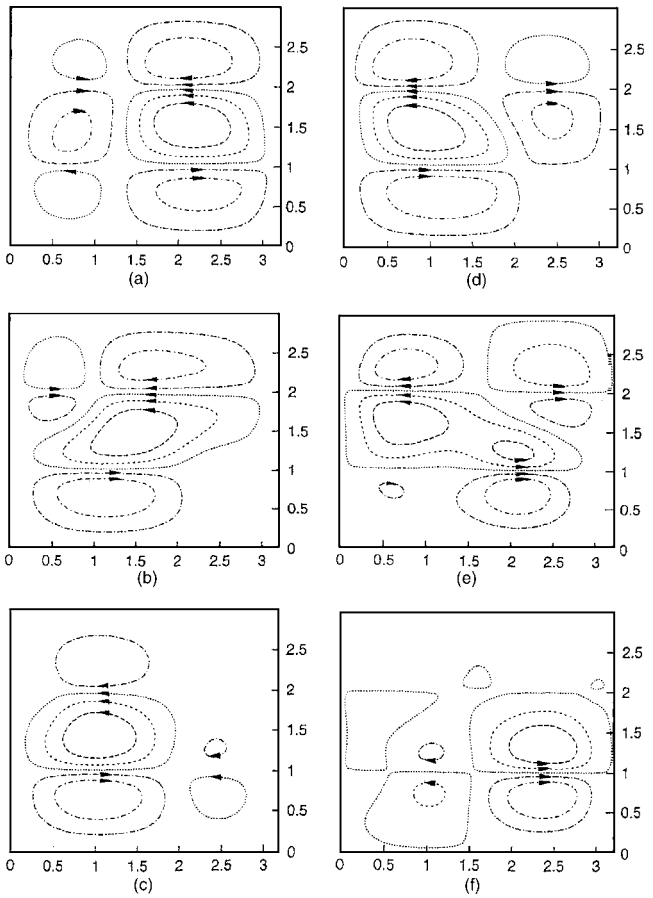

FIG. 4. (a)–(f) Streamlines for periodic oscillatory motion ($\epsilon=0.05$; $M=25\,000$).

Let us define the following integral quantities, characterizing the intensity of motion in the left or in the right half of the corresponding layer:

$$S_{l1}(t) = \int_{-L/2}^{0} dx \int_{0}^{1} dz\ \psi_1(x,z,t),$$

$$S_{r1}(t) = \int_{0}^{L/2} dx \int_{0}^{1} dz\ \psi_1(x,z,t), \tag{31}$$

$$S_{l2}(t) = \int_{-L/2}^{0} dx \int_{-1}^{0} dz\ \psi_2(x,z,t),$$

$$S_{r2}(t) = \int_{0}^{L/2} dx \int_{-1}^{0} dz\ \psi_2(x,z,t), \tag{32}$$

$$S_{l3}(t) = \int_{-L/2}^{0} dx \int_{-2}^{-1} dz\ \psi_3(x,z,t),$$

$$S_{r3}(t) = \int_{0}^{L/2} dx \int_{-2}^{-1} dz\ \psi_3(x,z,t). \tag{33}$$

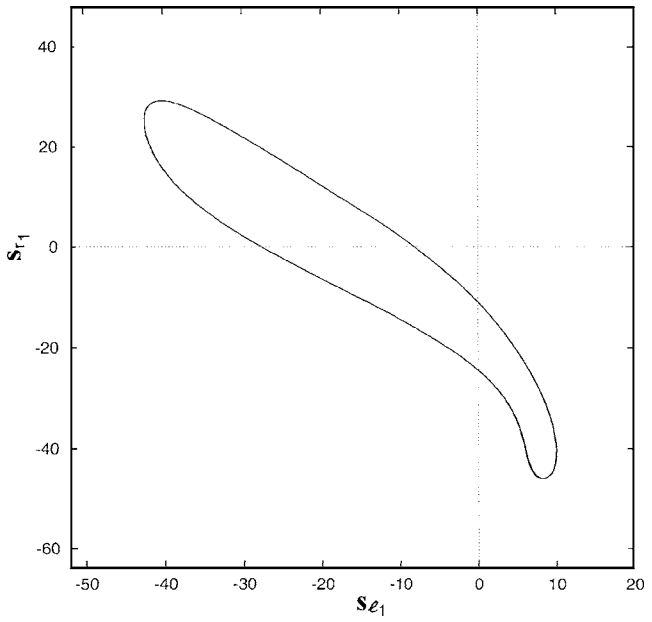

FIG. 5. Phase trajectory in variables S_{l1}, S_{r1}, for periodic asymmetric oscillatory motion ($\epsilon=0.05$; $M=25\,000$).

The time evolution of the quantities $S_{l,m}(t)$, $m=1,2,3$, shows that the oscillations are almost harmonic; the largest amplitude of oscillations is observed in the middle layer. For symmetric oscillations satisfying conditions (29), the integral quantities satisfy the relations

$$S_{l1}(t) = -S_{r1}(t), \quad S_{l2}(t) = -S_{r2}(t), \quad S_{l3}(t) = -S_{r3}(t). \tag{34}$$

The period of oscillations τ decreases with the growth of the Marangoni number M (see line 1 of Fig. 3).

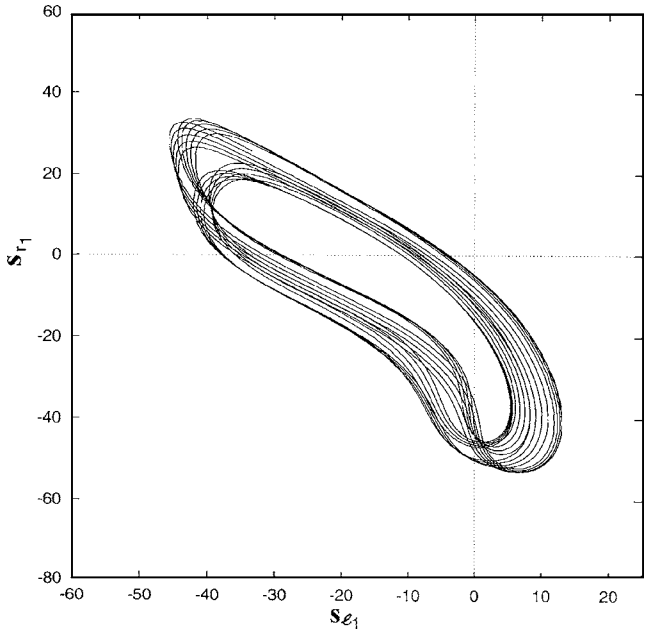

FIG. 6. Phase trajectory in variables S_{l1}, S_{r1}, for aperiodic oscillatory motion ($\epsilon=0.05$; $M=29\,000$).

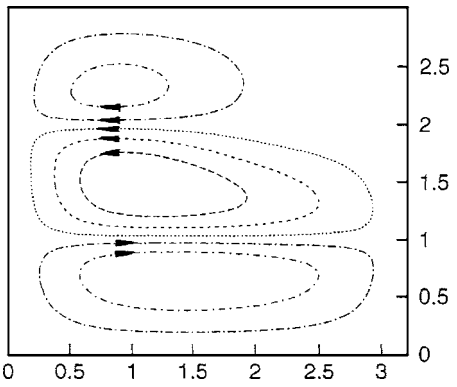

FIG. 7. Streamlines for stationary motion ($\epsilon=0.1$; $M=25\,000$).

If $M > M_*$, the symmetric oscillatory motion is unstable. A new, asymmetric, motion is developed through a period-doubling bifurcation. For this motion, the symmetry conditions (29) and (34) are violated. The time evolution of quantities $S_{l,m}(t)$, $m=1,2,3$, for the asymmetric motion is essentially nonsinusoidal. The period of oscillations decreases with increasing M (line 2 of Fig. 3). For larger values of M, the motion becomes aperiodic in time.

B. The case $\epsilon \neq 0$

Let us consider now the influence of a horizontal temperature gradient on structures described above. For any $\epsilon \neq 0$ the symmetry conditions (29) are violated and asymmetric oscillatory motion takes place in the system. The streamlines for this type of motion during the period of oscillations $0 < t < \tau$ are presented in Fig. 4. One can see that in comparison with the symmetric oscillatory motion the vortices have the tendency to become longer (cf. Figs. 2 and 4). The time evolution of quantities $S_{l,m}(t)$ $m=1,2,3$, for asymmetric

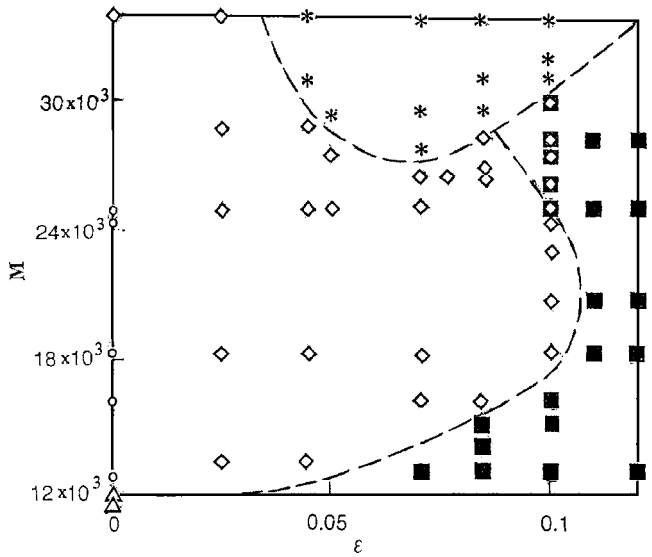

FIG. 8. Diagram of the flow regimes. △, equilibrium state; ○, periodic symmetric oscillations; ◇, periodic asymmetric oscillations; ■, stationary state; ∗, irregular asymmetric oscillations.

motion is essentially nonsinusoidal. The phase trajectory of asymmetric periodic oscillations in the variables (S_{l1}, S_{r1}), is shown in Fig. 5. The period of oscillations decreases with increasing M (lines 3 and 4 of Fig. 3). For larger values of M at a fixed value of ϵ, oscillations turn out to be aperiodic in time. The phase trajectory for the aperiodic motion is presented in Fig. 6. With an increase of ϵ at a fixed value of M, the asymmetric oscillatory motion disappears and a stationary structure with long cells in each fluid layer is preferentially formed in the system (Fig. 7). The results of the numerical simulations described above are summarized in the general diagram of regimes on the plane (ϵ, M) (see Fig. 8).

IV. CONCLUSION

The influence of the horizontal component of the temperature gradient on the Marangoni convection in a symmetric three-layer system 47v2 silicone oil–water–47v2 silicone oil has been investigated. The transitions between the nonlinear regimes of convection have been studied. It is shown that in a definite region of the parameter ϵ characterizing the horizontal component of the temperature gradient, regular asymmetric oscillations develop in the system. With an increase of ϵ at a fixed value of the Marangoni number, the asymmetric oscillatory motion becomes unstable and a stationary structure is formed preferentially in the system. A general diagram of the regimes is constructed.

[1] I. B. Simanovskii and A. A. Nepomnyashchy, *Convective Instabilities in Systems with Interface* (Gordon and Breach, London, 1993).
[2] S. Wahal and A. Bose, Phys. Fluids **31**, 3502 (1988).
[3] T. Doi and J. N. Koster, Phys. Fluids A **5**, 1914 (1993).
[4] P. Georis and J.-C. Legros, in *Materials and Fluids under Low Gravity*, edited by L. Ratke, H. Walter, and B. Feuerbacher (Springer, Berlin, 1996), p. 299.
[5] H. Groothuis and F. G. Zuiderweg, Chem. Eng. Sci. **12**, 288 (1960).
[6] I. B. Simanovskii, Physica D **102**, 313 (1997).
[7] A. A. Nepomnyashchy and I. B. Simanovskii, Phys. Rev. E **59**, 6672 (1999).
[8] A. Prakash, D. Fujita, and J. N. Koster, Eur. J. Mech. B/Fluids **12**, 15 (1993).
[9] A. Prakash and J. N. Koster, Eur. J. Mech. B/Fluids **12**, 635 (1993).
[10] A. Prakash and J. N. Koster, Int. J. Multiphase Flow **20**, 383 (1994).
[11] A. Prakash and J. N. Koster, Int. J. Multiphase Flow **20**, 397 (1994).
[12] I. Simanovskii, P. Georis, M. Hennenberg, S. Van Vaerenbergh, I. Wertgeim, and J.-C. Legros, in Proceedings of the Eighth European Symposium on Materials and Fluid Sciences in Microgravity, Brussels, Belgium, 1992, p. 729.
[13] Q. Liu and B. Roux, in Proceedings of the Eighth European Symposium on Materials and Fluid Sciences in Microgravity, Brussels, Belgium, 1992, p. 735.
[14] P. Georis, M. Hennenberg, I. Simanovskii, A. Nepomnyashchy, I. Wertgeim, and J.-C. Legros, Phys. Fluids A **5**, 1575 (1993).
[15] P. Georis, M. Hennenberg, G. Lebon, and J.-C. Legros, J. Fluid Mech. **389**, 209 (1999).
[16] I. Simanovskii, P. Georis, A. Nepomnyashchy, and J.-C. Legros, Phys. Fluids **15**, 3867 (2003).
[17] J. E. Weber, Int. J. Heat Mass Transfer **16**, 961 (1973).
[18] J. E. Weber, J. Fluid Mech. **87**, 65 (1978).
[19] R. E. Kelly, Adv. Appl. Mech. **31**, 35 (1994).
[20] S. H. Davis, Annu. Rev. Fluid Mech. **19**, 403 (1987).
[21] A. A. Nepomnyashchy, I. B. Simanovskii, and L. M. Braverman, J. Fluid Mech. **442**, 141 (2001).
[22] V. M. Shevtsova, I. B. Simanovskii, A. A. Nepomnyashchy, and J.-C. Legros, C. R. Mec. **333**, 311 (2005).